Discovery of Neutron-Rich Co and Fe Isotopes in $^{239}Pu(n_{th},f)$: Yields and Half-Lives

M. Bernas,[1] P. Armbruster,[2] S. Czajkowski,[1] H. Faust,[2] J. P. Bocquet,[3] and R. Brissot[3]

[1]*Institut de Physique Nucléaire, Orsay, France*

[2]*Institut Laue-Langevin, Grenoble, France*

[3]*Institut des Sciences Nucléaires, Grenoble, France*

(Received 3 May 1991)

Co and Fe isotopes have been identified in thermal-neutron-induced fission of ^{239}Pu. The yields of the very neutron-rich isotopes ^{69}Co, ^{68}Co, and ^{68}Fe were measured and their β-decay half-lives were obtained from time correlations between detection of the selected isotopes and of the β particles from their decay.

PACS numbers: 25.85.Ec, 27.50.+e

Fission has been known for a long time to provide the most neutron-rich isotopes. Recently, with ever improving separation techniques, very heavy Cu and Ni isotopes, up to ^{75}Cu and ^{74}Ni, have been identified in $^{235}U(n_{th},f)$ [1]. The decay scheme of ^{76}Cu was established [2] and the half-life of ^{78}Cu [3] was measured. More recently, the neutron closed-shell nucleus ^{79}Cu ($N=50$), with a neutron excess of 14 as compared with the heaviest stable Cu isotope, was discovered in ^{238}U fission induced by fast protons [4].

In a previous investigation we have measured systematically the asymmetric fragmentation of ^{235}U in the mass range between 80 and 70 for which the production yields were found to decrease from 10^{-3} to 10^{-8} [5]. The same experiment has recently been performed with ^{239}Pu [6]. Since the production yields are larger than for ^{235}U, ^{239}Pu thermal fission was selected in order to search for the very light masses $A=69$ and 68. In this paper, we show that fragments as light as iron with an excess of 10 to 12 neutrons are accessible through thermal fission.

Beyond the mere identification of new nuclear species, we have developed a method to measure their β-decay half-lives [7]. The comparison of this basic nuclear property with theoretical predictions provides constraints for nuclear and β-decay models, particularly when the isotopes studied are very far from stability and their properties difficult to extrapolate from previous data. Moreover, these values are required to understand the astrophysical r process synthesizing the elements beyond Fe. The isotopes under study are the heaviest ones created during this process. A knowledge of their half-lives will help to better define the astrophysical site, the conditions of neutron density, stellar temperature, and exposure time related to this process [8].

The experiment was performed using the recoil spectrometer Lohengrin at the high flux reactor of the Institut Laue-Langevin, Grenoble. A neutron flux of 5×10^{14} neutrons/cm^{2}s impinged on a 0.10 mg cm^{-2} target of ^{239}Pu of 99.99% isotopic purity, covered with a 0.25 mg cm^{-2} nickel foil to reduce plutonium sputtering.

Separated by Lohengrin, the fragments are focused on lines of a given A/q ratio (A being the atomic mass, q the ionic charge) with an A/q resolving power of 800 [9]. A 3-mm-wide slit, corresponding to this resolving power, allows a full transmission with a good suppression of neighboring lines. Along these lines the ions of different energies are dispersed, the 70-mm length of the slit giving a 1-MeV energy acceptance. A two-stage ionization chamber [10] measures the energy E with a 1% accuracy, providing unambiguously the ionic charge and mass number. In the first stage of the chamber an energy-loss measurement, ΔE, gives the atomic number of the fragments. The properties of the experimental setup are illustrated on the scatter plots obtained for $A/q=69/17$ and $A/q=68/18$ (Fig. 1). The performances of this setup enable us to single out fission yields of 10^{-9}; but the small solid angle, the energy, and charge state selection limit the col-

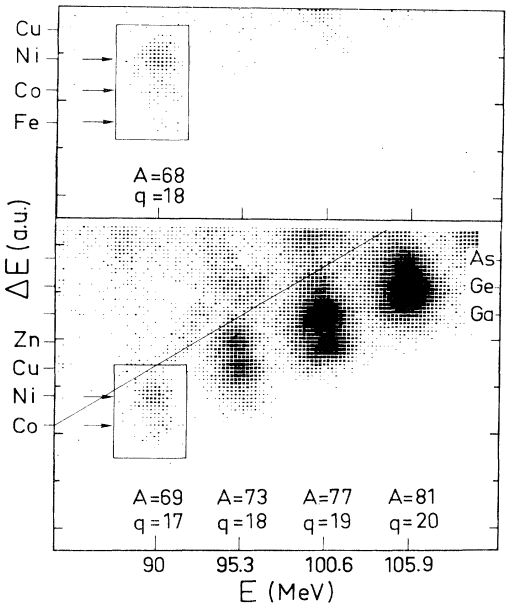

FIG. 1. ΔE-E scatter plots accumulated over 50 h ($A/q=68/18$) and 40 h ($A/q=69/17$). At low values of ΔE (i.e., low Z) four groups of ions, associated with close A/q values, are separated with the help of energy measurement. The top part of the plot (above the diagonal line) shows contamination with heavier fragments, the charge states of which have been changed in atomic collisions in the space between the two fields of the spectrometer. The area of interest, that of low ΔE, is background free. The isotopic separation improves with decreasing Z. From the known isobaric distribution of the mass lines $A=81$ and $A=77$, we calibrate the ΔE axis in terms of atomic numbers.

lection efficiency to 10^{-7}. One charge state and the kinetic energy of the fragments were selected referring to the ionic charge and energy distributions measured for $^{235}U(n_{th},f)$ [11]. The aim was to optimize the counting rate of the isotope under study together with a low β background rate, i.e., keeping the contamination from heavier fragments under control.

The β-decay half-life is obtained from time correlations between the identified fragments and the β particles counted thereafter. At the very end of their trajectories the fragments are implanted into one of eight planar Si detectors of $10\times10\times0.5$ mm^3 where the few MeV residual energy of the fragments and the energy-loss signals of the subsequent β are measured. Since fragments are implanted only on the surface layer of the Si detector, the β detection efficiency ε is limited to 50% at maximum. The 13-keV β energy resolution of those Si detectors allows a clear discrimination of signals from the electronic noise. The continuous spectra of β energy loss show a wide peak, with a maximum at 170 keV. A low-energy threshold is set at 50 keV to eliminate noise and x rays produced by the Lohengrin condenser. The correlation efficiency, accounting for threshold, electronics, and data processing, was evaluated systematically on the β decay of ^{96}Sr ($T_{1/2}=1$ s). It was found to be (40 ± 5)%.

A β background rate b of 0.2 to 0.4 s^{-1} per detector was counted together with 0.5 to 1 fragment per second in the chamber. The β rate is due to the many heavier fission fragments entering the chamber, each emitting 2 to 4 β particles before reaching the line of stability and to the high radiation level close to the reactor. This background rate limits the largest measurable half-life to 2 s. Therefore half-lives of Ni isotopes lighter than 71 were not accessible.

The knowledge and control of the stability of the background rate is crucial for time correlations to be reliable. This rate was continuously registrated during the measurements. It was also evaluated from the Poisson distribution of time gaps between the fragments and the previous uncorrelated β particle.

The mass and elemental yields for masses 73, 69, and 68 have been determined in reference to the known $A=82$ mass yield [6]. Under the same experimental conditions, we have compared counting rates for the lines $A/q=68/18$ and $A/q=82/17$ at a spectrometer energy of 90 MeV, that is, 97-MeV fission energy when corrected for energy losses in the target and in the covering foil. The counting rate of mass 82 was multiplied by the ratio of ionic yields 19/17 at the same mass and same energy as in the fission of ^{235}U [11]. The two partial rates obtained for $A=68$ and 82, both close to the maximum of the charge distribution, were assumed to be proportional to mass yields integrated over q and E. The yield for mass 69 (73) was compared to that for mass-68 on the basis of the counting rates at charge states 17 (18) and energy of 90 MeV (and 95.3 MeV), respectively (see Fig. 1). The error so introduced is smaller by far than uncertainties resulting from the counting statistics. The results (Table I) are compared in Fig. 2 with the mass yield distribution extrapolated by Wahl [12] from the data on the heavy partner, in mass range $A=170$–160. Most of the mass yields measured previously agree with this evaluation, except for mass 70, the yield of which was found to be 4 times larger than predicted [6]. In this work the mass-68 yield is also found to be larger than predicted, by a factor of 8. Both differences are related to odd-even effects combined with the shell closure at $Z=28$. Nickel is the dominating element from mass 72 down to mass 68. Within each mass line, the isotopic yields are provided by the analysis of projected spectra along the energy-loss axis (see Fig. 1). Obtained for one selected ionic state, the yields are summed over the other relevant states by using the known charge distributions [11].

TABLE I. $Pu(n_{th},f)$ measured mass yield and isotopic yields.

A	Mass yield (%) $Pu(n_{th},f)$	Relative isotopic yield (%) Fe	Co	Ni	Cu	Zn
82	19×10^{-2} [a]					
73	$(15\pm3)\times10^{-5}$			3.8	55	41.2
69	$(11\pm2)\times10^{-6}$		20	79		
68	$(6.6\pm1.3)\times10^{-6}$	3.8	10.7	85.5		

[a]Reference [6].

Compared with the results obtained for $^{235}U(n_{th},f)$ in the same mass range, the slope of decreasing yields is less steep, and the Z distribution is found to be wider and shows less odd-even effects. These differences show once more the surprisingly strong dependence of the fission process on the dynamics, changing from one fissioning nucleus to another.

The probability for counting β particles at time t after the detection of the fragment and the probability of finding the very first β after the fragment at a time t are

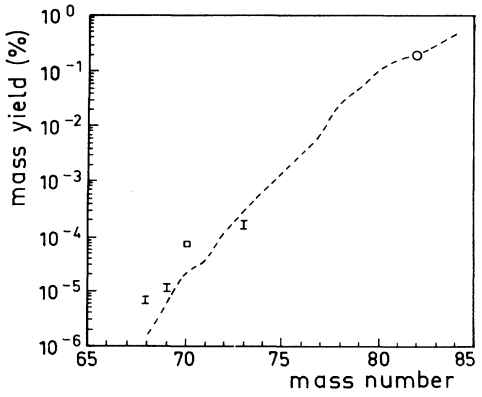

FIG. 2. Mass yield distribution in $^{239}Pu(n_{th},f)$ as given by Wahl [12] (dashed line). The measurements are normalized on the mass-82 yield [6] (open circle). The yields presently measured (vertical bars) are larger than predicted for $A=68$ as found by Dietz [6] for $A=70$ (square) due to Ni shell closure.

TABLE II. Conditions for half-life measurements. Comparison of the resulting values with the calculated ones.

Isotope	Counting rate (h^{-1})	Number of events detected	Half-life (s)	Calculated half-life (s) Revised gross theory [14]	Microscopic theories [15]	[16]
^{69}Co	1.52	175	0.27 ± 0.05	0.73	0.68	0.071
^{68}Co	0.43	80	0.18 ± 0.10	0.80	0.81	0.29
^{68}Fe	0.15	29	0.10 ± 0.06	0.37	0.42	0.16

given respectively by

$$\rho(\lambda,t) = b + \varepsilon\lambda e^{-\lambda t}, \quad \rho_1(\lambda,t) = \varepsilon(b+\lambda)e^{-(b+\lambda)t} + (1-\varepsilon)be^{-bt},$$

where λ is the decay constant. If the daughter nucleus decays with a constant λ_f, the corresponding β can be detected as well and the probability densities become

$$\rho(\lambda,\lambda_f,t) = \rho(\lambda,t) + \varepsilon\frac{\lambda\lambda_f}{\lambda-\lambda_f}(e^{-\lambda_f t} - e^{-\lambda t})$$

and

$$\rho_1(\lambda,\lambda_f,t) = \rho_1(\lambda,t) + \varepsilon(1-\varepsilon)e^{-bt}\left\{\frac{\lambda\lambda_f}{\lambda-\lambda_f}\left[\left(1+\frac{b}{\lambda_f}\right)e^{-\lambda_f t} - \left(1+\frac{b}{\lambda}\right)e^{-\lambda t}\right] - b\right\}.$$

The measured time distribution of β particles over a time t_c following the selected fragments (denoted I) is expressed by $\Delta N_\beta = N_F \rho \Delta t$, where N_F is the number of fragments. Similarly the distribution of the time gaps between each selected fragment and the next β (II) is given by $\Delta N_\beta = N_F \rho_1 \Delta t$. The value of λ can be deduced either from a χ^2 minimization or by a maximum-likelihood procedure. This last analysis is actually more appropriate, due to the small number of correlations (see Table II) and the occurrence of a significant β background.

For ^{69}Co the four evaluations are compatible within their accuracies and they give a mean value of 0.27 ± 0.05 s.

For ^{68}Co and ^{68}Fe, the numbers of events are very low and only the maximum-likelihood analysis of distribution (I) is appropriate. The ^{68}Co correlations were analyzed first, since the half-life of the daughter nucleus ^{68}Ni is known [13] to be long (19 s) compared with the value searched for: Then statistical uncertainties due to the daughter decay are reduced [compare Figs. 3(b) and 3(c)]. Furthermore the ^{68}Co fragments are 3 times more abundant than the ^{68}Fe ones. A half-life of 0.18 ± 0.10 s was found; the large uncertainty comes from the variation in the background and in the detection efficiency in the different runs. The 29 correlations observed for ^{68}Fe were analyzed similarly, but there the contribution of daughter decays is significant and the error in the ^{68}Co result propagates to ^{68}Fe. A $T_{1/2}$ value of 0.10 ± 0.06 s is obtained. Both results are illustrated in Fig. 3.

Among the 29 time sequences of β signals following the implantation of ^{68}Fe, 6 could be assigned to the detection of both β particles of the decay chain, followed by a β from the background with appropriate time gaps.

This number of detected chains is compatible with the expected number, $N_F\varepsilon^2$, and the time sequences provide mean times, and therefore half-lives, in excellent agreement with the values obtained above.

In spite of their low accuracy—notice that ^{68}Fe has four neutrons more than the heaviest isotope of measured half-life—these experimental results offer a way to test nuclear models. Predicted β-decay half-lives scatter appreciably. The revised gross theory of β decay [14] and microscopic calculations [15] lead to half-lives in agreement with the values we have measured previously for neutron-rich Ni isotopes [7]. For the two Co isotopes under study, the calculated half-lives are both larger than the experimental ones by a factor of 4. Recent microscopic calculations based on quasiparticle random-phase approximation (RPA) [16] have improved the overall agreement with data for neutron-rich isotopes between Ni and Zn [17]. This improvement is confirmed here for ^{68}Co and ^{68}Fe. Only the odd-even ^{69}Co is predicted as decaying more rapidly, by a factor of 4. A deformation can occur for this Co isotope, which may have been underestimated by the RPA calculation. Reducing the overlap of the wave functions of ^{69}Co with ^{69}Ni would slow the β decay. This assumption is corroborated by the presence of a low-energy shape isomer in the $N=40$ ^{68}Ni isotope [18].

In the field of nucleosynthesis, the present findings (as well as those of [2–4] and [7,8]) concern isotopes located along the first steps of the r process, from ^{56}Fe to ^{80}Zn. The readjustment of the Co and Fe half-lives to shorter values will shift the r path previously calculated [19] toward larger Z and thus can modify the calculation of the mass distribution due to the r process.

After fifty years of intensive studies, thermal fission

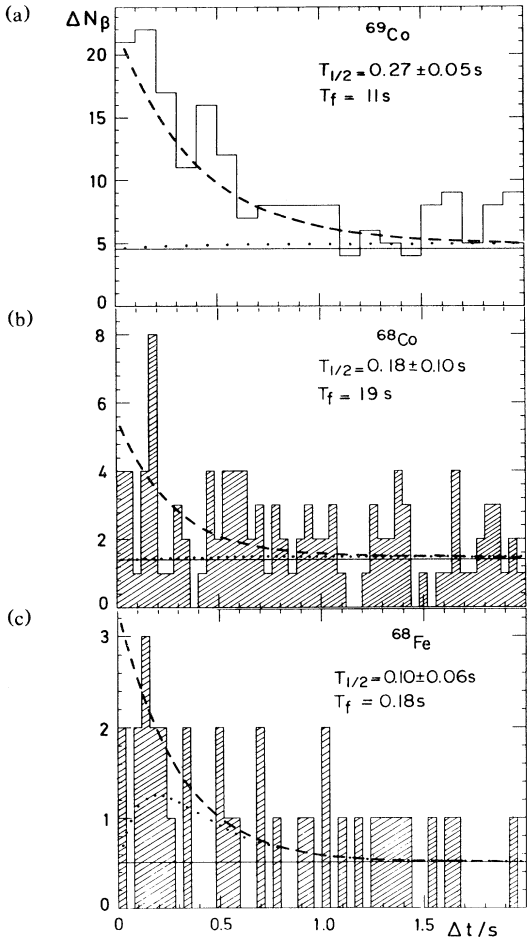

FIG. 3. Illustrations of the time correlation spectra obtained for the three new isotopes of ^{69}Co, ^{68}Co, and ^{68}Fe. The curves are calculated with the half-lives obtained with the maximum-likelihood procedure. Solid curve, background; dotted curve, background plus daughter decay of half-life T_f; dashed curve, calculated with the value found for $T_{1/2}$.

continues to reveal new isotopes. The discovered Co and Fe fragments are not only the lightest fragments ever seen in fission, they are also the most neutron-rich isotopes of these elements ever reported. They are found with an extremely low yield. Fission remains the most appropriate process to generate neutron-rich isotopes, but the present experiment suffers from the low collection efficiency, 10^{-7}. This lack of efficiency could be overcome by taking advantage of the kinematic forward focusing of products from ^{238}U Coulomb dissociation at high energies, using beams delivered by a heavy-ion synchrotron and separated by a recoil separator. The expected rate would then increase by 2 orders of magnitude. This increase would allow nuclei further from stability, by at least two neutrons, to be reached and $^{78}_{28}Ni_{50}$, the spectroscopy of which is of utmost interest, will come within the scope of such investigations.

[1] P. Armbruster *et al.*, Europhys. Lett. **47**, 793 (1987).
[2] J. A. Winger *et al.*, Phys. Rev. C **42**, 954 (1990).
[3] E. Lund *et al.*, in *Proceedings of the Fifth International Conference on Nuclei Far from Stability,* edited by I. S. Towner, AIP Conf. Proc. No. 164 (AIP, New York, 1988), p. 578.
[4] K. L. Kratz *et al.*, Verh. Dtsch. Phys. Ges. **E2.5**, 438 (1991).
[5] J. L. Sida *et al.*, Nucl. Phys. **A502**, 233 (1989).
[6] W. Dietz, J. O. Denschlag, and H. R. Faust (to be published).
[7] M. Bernas *et al.*, Z. Phys. A **337**, 41 (1990).
[8] K. L. Kratz, in *Proceedings of the Workshop on Nuclear Astrophysics,* Lecture Notes in Physics Vol. 287 (Springer-Verlag, Berlin, 1987).
[9] E. Moll *et al.*, Nucl. Instrum. Methods **123**, 615 (1975).
[10] J. P. Bocquet, R. Brissot, and H. R. Faust, Nucl. Instrum. Method Phys. Res., Sect. A **267**, 466 (1988).
[11] J. L. Sida, thèse, Université de Paris XI, Orsay (unpublished); (to be published).
[12] A. C. Wahl, At. Data Nucl. Data Tables **39**, 1 (1988).
[13] W. D. Schmidt-Ott *et al.*, in *Proceedings of the Fifth International Conference on Nuclei Far from Stability* (Ref. [3]), p. 365.
[14] T. Tachibana, M. Yamada, K. Nakata, Report of Sciences and Engineering Research Laboratory, Wasada University, 88-4, 1988 (unpublished).
[15] H. V. Klapdor, J. Metzinger, and T. Oda, At. Data Nucl. Data Tables **31**, 81 (1984).
[16] A. Staudt *et al.*, At. Data Nucl. Data Tables **44**, 79 (1990).
[17] M. Bernas *et al.*, in *Proceedings of the Twenty-First International Summer School on Nuclear and Atomic Physics with the Accelerators of the Ninetees* (Soltan Institute for Nuclear Physics, Poland, 1990).
[18] M. Bernas *et al.*, Phys. Lett. **113B**, 279 (1982); J. Phys. (Paris), Lett. **45**, 851 (1984).
[19] K. L. Kratz, Rev. Mod. Astron. **1**, 184 (1988).